Oncogene (2004) 23, 379–385

www.nature.com/onc

The differential impact of p16^{INK4a} or p19^{ARF} deficiency on cell growth and tumorigenesis

Norman E Sharpless*,[1], Matthew R Ramsey[1], Periasamy Balasubramanian[1], Diego H Castrillon[2,3,4] and Ronald A DePinho[2]

[1]*Departments of Medicine and Genetics, Lineberger Cancer Center, CB# 7295, The University of North Carolina School of Medicine, Chapel Hill, NC 27599-7295, USA;* [2]*Departments of Adult Oncology, Medicine and Genetics, Dana-Farber Cancer Institute and Harvard Medical School, Boston, MA, USA;* [3]*Department of Pathology, Brigham and Women's Hospital, Harvard Medical School, Boston, MA, USA*

Mounting genetic evidence suggests that each product of the *Ink4a/Arf* locus, p16^{INK4a} and p19^{ARF}, possesses tumor-suppressor activity (Kamijo *et al*., 1997; Krimpenfort *et al*., 2001; Sharpless *et al*., 2001a). We report the generation and characterization of a p19^{ARF}-specific knockout allele (*p19^{ARF}−/−*) and direct comparison with mice and derivative cells deficient for p16^{INK4a}, both p16^{INK4a} and p19^{ARF}, and p53. Like *Ink4a/Arf−/−* murine embryo fibroblasts (MEFs), *p19^{ARF}−/−* MEFs were highly susceptible to oncogenic transformation, exhibited enhanced subcloning efficiency at low density, and resisted both RAS- and culture-induced growth arrest. In contrast, the biological profile of *p16^{INK4a}−/−* MEFs in these assays more closely resembled that of wild-type cells. *In vivo*, however, both *p19^{ARF}−/−* and *p16^{INK4a}−/−* animals were significantly more tumor prone than wild-type animals, but each less so than *p53−/−* or *Ink4a/Arf−/−* animals, and with differing tumor spectra. These data confirm the predominant role of p19^{ARF} over p16^{INK4a} in cell culture-based assays of MEFs, yet also underscore the importance of the analysis of tumor suppressors across many cell types within the organism. The cancer-prone conditions of mice singly deficient for either p16^{INK4a} or p19^{ARF} agree with data derived from human cancer genetics, and reinforce the view that both gene products play significant and nonredundant roles in suppressing malignant transformation *in vivo*.

Oncogene (2004) **23,** 379–385. doi:10.1038/sj.onc.1207074

Keywords: Rb; p14^{ARF}; p53; cdkn2a

Introduction

The *Ink4a/Arf* locus encodes two proteins, p16^{INK4a} and p14^{ARF} (p19^{ARF} in the mouse), in overlapping reading frames which are commonly codeleted in a large variety of human cancers (reviewed in Lowe and Sherr 2003). Human genetic data suggest that both *Ink4a/Arf* products are important tumor-suppressor proteins (Hussussian *et al*., 1994; Kamb *et al*., 1994; FitzGerald *et al*., 1996; Randerson-Moor *et al*., 2001; Rizos *et al*., 2001; Hewitt *et al*., 2002). Likewise, mice lacking both p16^{INK4a} and p19^{ARF} (*Ink4a/Arf−/−*), lacking p16^{INK4a} only (*p16^{INK4a}−/−*), or p19^{ARF} only (*p19^{ARF}−/−*) are prone to tumors spontaneously and are sensitive to carcinogens, albeit with apparent differences in latency and tumor spectra (Serrano *et al*., 1996; Kamijo *et al*., 1997; Krimpenfort *et al*., 2001; Sharpless *et al*., 2001a). From these data, it appears that the unusual genomic structure of *Ink4a/Arf* allows for concomitant inactivation of two archetypal tumor-suppressor pathways, Rb and p53, through deletion of this single locus.

While both proteins play a role in culture-induced growth arrest, the relative roles of each vary in a cell-type- and species-specific manner. For example, under certain conditions, p16^{INK4a} accumulates in serially passaged primary human cells, and immortalization of these cells requires p16^{INK4a} loss, generally through promoter methylation (Brenner *et al*., 1998; Foster *et al*., 1998; Huschtscha *et al*., 1998; Kiyono *et al*., 1998; Rheinwald *et al*., 2002; Sviderskaya *et al*., 2003). On the other hand, no clear role for p14^{ARF} in the growth arrest of cultured human cells has been consistently demonstrated (Munro *et al*., 1999; Wei *et al*., 2001; Rheinwald *et al*., 2002). In murine cells, p16^{INK4a} appears to participate in culture-induced arrest of a few cell types (e.g. astrocytes (Bachoo *et al*., 2002), macrophages (Randle *et al*., 2001), and v-abl transduced lymphocytes (Sachs *et al*., in submission)), but p19^{ARF} appears more important in most of these cases. In MEFs, for example, p19^{ARF} loss is sufficient for immortalization, while loss of p16^{INK4a} is not (Kamijo *et al*., 1997; Krimpenfort *et al*., 2001; Sharpless *et al*., 2001a). Likewise, RAS-induced growth arrest requires p16^{INK4a}–Rb in human cells (and not ARF), while the opposite appears true in MEFs (Kamijo *et al*., 1997; Serrano *et al*., 1997; Zhu *et al*., 1998; Krimpenfort *et al*., 2001; Sharpless *et al*., 2001a; Wei *et al*., 2001; Brookes *et al*., 2002; Huot *et al*., 2002). These cell-type and species discrepancies are presently unexplained. It appears, however, that a somewhat generic feature(s) of cell culture ('oncogenic stress') is capable of inducing both p16^{INK4a} and ARF expression in a multitude of cell types (Sherr and DePinho, 2000). It is not known, however, if the characteristics of a nascent

*Correspondence: NE Sharpless; E-mail: NES@med.unc.edu
[4]Current address: Department of Pathology, University of Texas Southwestern Medical Center, Dallas, TX, USA
Received 18 June 2003; revised 31 July 2003; accepted 1 August 2003

tumor that induce p16^{INK4a} and ARF expression are related to those stimuli that induce the *Ink4a/Arf* locus in culture.

Despite a number of previous studies of isolated or combined p16^{INK4a} and p19^{ARF} deficiency (Serrano *et al*., 1996; Kamijo *et al*., 1997; Krimpenfort *et al*., 2001; Sharpless *et al*., 2001a; reviewed in Sherr (2001), comparison of these series is difficult because of differences in genetic background, allele design, housing environment, pathologic characterization, etc. Here, we report the comparison of these mice and derivative cells to those lacking p16^{INK4a} only (*p16^{INK4a}−/−*), both p16^{INK4a} and p19^{ARF} (*Ink4a/Arf−/−*), and p53 (*p53−/−*), all in a similar genetic background, and followed and analysed in common facilities by a single group of investigators over the same period.

Results

Mice lacking p19^{ARF} were generated using standard gene-targeting techniques, with Cre-mediated excision of the neomycin selection cassette (Figure 1a) in a manner similar to *p16^{INK4a}−/−* mice (Sharpless *et al*., 2001a). Homologous integration and correct Cre-mediated excision were determined by Southern analysis (Figure 1b) and PCR (Figure 1c), respectively. This targeting strategy generated a premature stop codon in exon 1*β*, leaving the *cis*-regulatory elements of *p19^{ARF}* and *p16^{INK4a}* unperturbed. Fibroblasts from *p19^{ARF}−/−* embryos demonstrated loss of p19^{ARF} by Western blotting using a C-terminal antibody (Figure 1d), and neither p53 nor its downstream target p21 were stabilized by serial passage in these cells consistent with their functional deficiency of p19^{ARF} (Figure 1d and e). In contrast to a previously described p19^{ARF}-specific KO which retains the neomycin selection cassette at the locus (Kamijo *et al*., 1997), MEFs from these animals demonstrated normal p16^{INK4a} expression at early passage (Figure 1d), although p16^{INK4a} expression was greater at later passages (e.g. P9 in Figure 1d), presumably because of the enhanced proliferation of *p19^{ARF}−/−* cells at these passages.

Embryo fibroblasts from *p19^{ARF}−/−* animals were compared to those from *p19^{ARF}+/+* littermates, as well as those from *p16^{INK4a}−/−* and *Ink4a/Arf−/−* embryos. The growth of *p19^{ARF}−/−* MEFs was indistinguishable from that of *Ink4a/Arf−/−* cells when assayed by 3T9 assay, while *p16^{INK4a}−/−* MEFs grew with kinetics more similar to that of wild-type MEF cultures (Figure 2a). In *p19^{ARF}+/+* cells, nucleolar p19^{ARF} expression increased with serial passage and was only rarely detected in BRDU+ cells (Figure 2b). Although this same trend was noted in *p16^{INK4a}−/−* MEFs, lines from this background more frequently harbored cells expressing both BRDU and p19^{ARF} (6% double positive in *p16^{INK4a} +/+* versus 13% in *p16^{INK4a}−/−* at passage 5; $P<0.01$). This observation suggests that a minority of *p16^{INK4a}−/−* cells continued to proliferate in the setting of detectable p19^{ARF} expression. While this small population of cells did not markedly influence growth as measured by a 3T9 assay (Figure 2a), this persistent proliferation may contribute to the increased propensity to escape of culture-induced growth arrest documented previously in *p16^{INK4a}−/−* MEFs (Sharpless *et al*., 2001a).

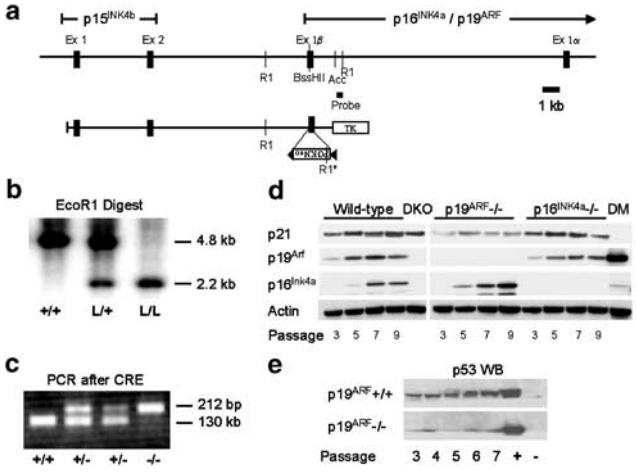

Figure 1 (**a**) Targeting strategy for p19^{ARF}. Transfected ES cells were screened for homologous recombination using a 250 bp *Apa*L1-*Eco*R1 probe external to the targeting vector. The selection cassette was excised by Cre-mediated recombination, to generate a null allele without disturbing the *cis*-regulatory elements of p19^{ARF}. (**b**) Southern analysis of mice of the indicated p19^{ARF} genotype. *Eco*R1-digested DNA was probed as described. An introduced *Eco*R1 site in the PGK-Neo cassette yields a smaller fragment from the targeted allele. L = targeted allele prior to Cre-mediated excision. (**c**) PCR screening of tail DNA from mice of the indicated genotypes. Primers flank the remnant LoxP site in the targeted allele. The targeted allele is 82 bp larger as the targeting strategy deletes 2 bp of WT DNA, and adds 84 bp of exogenous DNA (LoxP site + remnant DNA from the cloning sequences). (**d**) Western blot for p16^{INK4a}, p19^{ARF}, and p21 in MEFs of the indicated genotypes at the indicated passage number. The p53 target p21 is not induced in *p19^{ARF}−/−* cells. DKO = *Ink4a/Arf−/−* cells at late passage (>10). DM = 3T3DM cells (Olson *et al*., 1993). (**e**) p53 is not stabilized by serial passage in *p19^{ARF}−/−* cells. + indicates an *Ink4a/Arf−/−* melanoma cell line that overexpresses p53 (Bardeesy *et al*., 2001), − indicates *p53−/−* MEFs

Figure 2 (**a**) 3T9 assay of *p16^{INK4a}−/−*, *p19^{ARF}−/−*, *Ink4a/Arf−/−*, and wild-type MEFs. Wild-type embryo lines were derived from the littermates of *p19^{ARF}−/−* and *p16^{INK4a}−/−* embryos. Results are the average of at least 15 lines per genotype (68 lines total); all lines that had not senesced by passage 20 were immortal. (**b**) Immunofluorescence of wild-type MEFs at passages 5 and 11. BRDU staining (a marker of DNA synthesis) demonstrates a pan-nuclear pattern, while p19^{ARF} staining in nucleolar only (bright punctuate dots). Expression of p19^{ARF} correlates with cell cycle arrest, with only rare BRDU+ cells demonstrating detectable p19^{ARF}. (**c**) Myc-Ras transformation assay. *p19^{ARF}−/−* and *Ink4a/Arf−/−* MEFs are more transformable by H-Ras alone or by c-Myc and H-Ras in combination ($P<0.01$ for both *p19^{ARF}−/−* and *Ink4a/Arf−/−* cells compared pairwise with either *p16^{INK4a}−/−* or wild-type cells, at least three transfections per genotype analysed). (**d**) Low-density seeding assay. Crystal violet stained foci were counted 14 days after seeding 300 cells per six-well plate. *p19^{ARF}−/−* and *Ink4a/Arf−/−* MEFs formed significantly more foci than wild-type or *p16^{INK4a}−/−* cells ($P<0.01$ for both *p19^{ARF}−/−* and *Ink4a/Arf−/−* cells compared pairwise with either *p16^{INK4a}−/−* or wild-type cells, at least 24 wells per genotyped counted)

Likewise, transformation by Ras (with or without Myc, Figure 2c) and growth at low density (Figure 2d) were markedly enhanced by loss of $p19^{ARF}$, while the effect of $p16^{INK4a}$ deficiency in these assays was more modest. The increase in foci formation seen in $p16^{INK4a}-/-$ cells relative to $p16^{INK4a}+/+$ was statistically significant ($P<0.02$ for both Ras and Myc + Ras), but several fold lower than the difference seen between $p19^{ARF}+/+$ and $p19^{ARF}-/-$ cells, even after normalizing for the enhanced transfection efficiency of $p19^{ARF}-/-$ cells. No difference in growth at low density was noted between $p16^{INK4a}+/+$ and $-/-$ cells. Also, transduction of activated H-Ras induced p53 expression and growth arrest in wild-type and $p16^{INK4a}-/-$ cells, but not in $p19^{ARF}-/-$ cells (not shown). As reported previously (Krimpenfort *et al*., 2001; Sharpless *et al*., 2002), $p16^{INK4a}-/-$ cells accumulated to higher density after 3 weeks in culture without passaging. MEFs lacking $p19^{ARF}$, however, accumulated to normal density in this assay, consistent with the finding that culture under these conditions attenuates $p19^{ARF}$, but not $p16^{INK4a}$, expression (Sharpless *et al*., 2002). These data confirm that $p19^{ARF}$ is the dominant effector of MEF 'senescence' in response to serial passage or oncogenic RAS overexpression. In contrast, $p16^{INK4a}$ only modestly contributes to the growth characteristics of MEFs, and then only when highly expressed (e.g. after prolonged periods in culture) or in the setting of attenuated $p19^{ARF}$ expression (e.g. after prolonged culture at confluence).

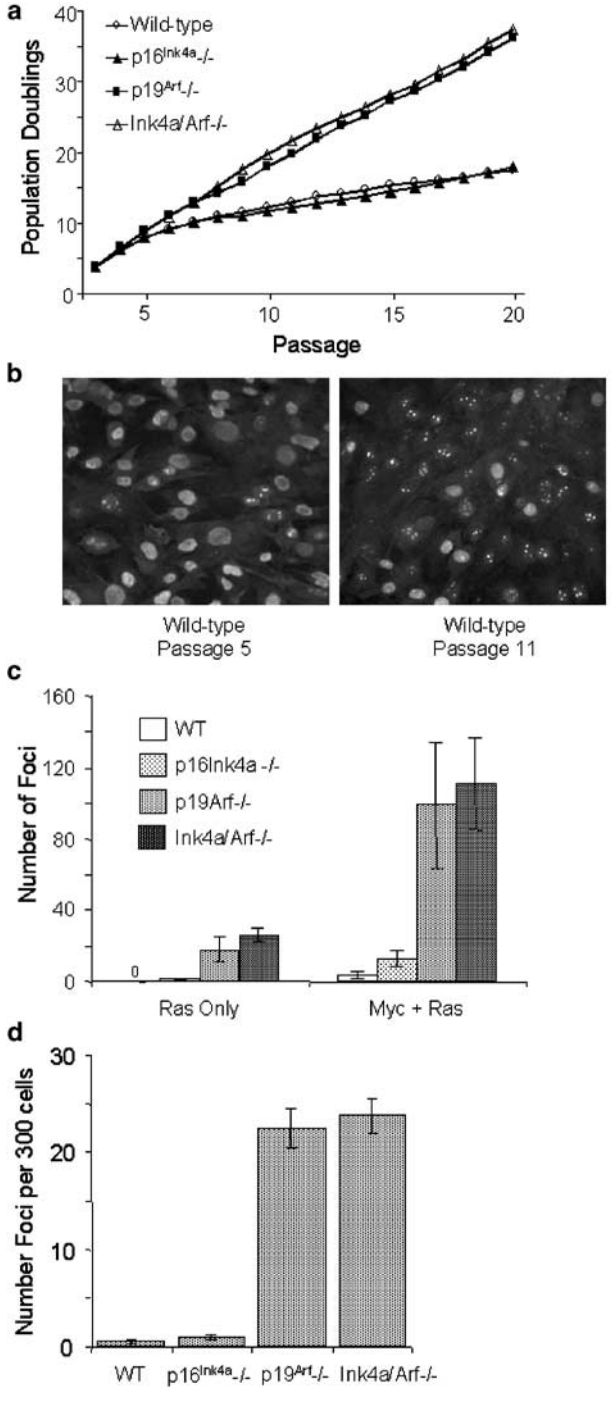

To assess the effects of $p19^{ARF}$ loss *in vivo*, we generated cohorts by intercrossing $p19^{ARF}+/-$ animals lacking the Cre-deletor transgene, and monitored these mice for the analysis of spontaneous and DMBA-induced tumor incidence. As previously reported (Kamijo *et al*., 1997, 1999), $p19^{ARF}-/-$ animals were significantly more tumor prone than $p19^{ARF}+/+$ littermates ($P<0.001$ for both spontaneous and carcinogen-induced tumors, Figure 3a and b). In comparison, mice lacking $p19^{ARF}$ appeared modestly more prone to spontaneous tumors than $p16^{INK4a}-/-$ mice, but significantly less tumor prone than *Ink4a*/*Arf*$-/-$ or *p53*$-/-$ mice (Figure 3a). For example, four of 41 $p19^{ARF}-/-$ mice survived >80 weeks, whereas *Ink4a*/*Arf*$-/-$ mice in this background seldom survive over a year (Figure 3a; Artandi *et al*., 2002; Sharpless *et al*., 2001b). Spontaneous or DMBA-induced tumors from $p19^{ARF}-/-$ mice were further analysed for $p16^{INK4a}$ expression. Thymic lymphomas (two of two) as well as a subset of soft-tissue sarcomas (two of four) and DMBA-induced lung nodules (one of three) demonstrated the expression of $p16^{INK4a}$ by Western analysis (not shown), while the remaining tumors showed no significant expression. This is in accord with results from a transgenic model of melanoma in $p19^{ARF}-/-$ mice, where the majority of tumors were shown to harbor a detectable lesion of the $p16^{INK4a}$-Rb pathway, most commonly loss of $p16^{INK4a}$ expression (Sharpless *et al*., 2003). These data confirm that $p19^{ARF}$ is a *bona fide* tumor suppressor, but also strongly suggest that the *Ink4a*/*Arf* locus encodes additional tumor-suppressor activity represented by $p16^{INK4a}$.

The tumor spectrum of $p19^{ARF}-/-$ animals was more similar to *p53*$-/-$ than $p16^{INK4a}-/-$ or *Ink4a*/*Arf*$-/-$ mice in a comparable genetic background (Table 1). The most common tumor in $p19^{ARF}-/-$ mice was a lymphocytic lymphoma of the thymus and/or lymph nodes. Animals lacking $p19^{ARF}$ also developed an increased incidence of spindle cell neoplasms (most likely soft tissue sarcomas, see Sharpless *et al*., 2001a, 2002), and carcinomas, particularly of the lung. The latter is of particular interest as spontaneous epithelial

tumors are not frequently detected in *Ink4a/Arf*−/−, *p53*−/− or $p16^{INK4a}$−/− mice. While FVB mice are predisposed to lung tumors (Festing, 1998), a similar increase in carcinoma has also been observed in mice lacking $p19^{ARF}$ in a different genetic background (B6/129) (Kamijo *et al*., 1997, 1999). Although a few mice demonstrated neurologic phenotypes (e.g. hind-limb paralysis, seizures), 1 mm sectioning of the brain of these animals did not reveal any glial tumors ($n=12$, $p19^{ARF}$+/− or −/− mice examined). Three of the six mice with hind-limb paralysis demonstrated osteosarcoma of the spine, and one animal with circling behavior exhibited a nonmalignant cerebral arteriovenous malformation with hemorrhage. In contrast, mice lacking *Ink4a/Arf*−/− predominantly develop a widely disseminated histiocytic tumor involving the spleen, peripancreatic and other lymph nodes or other sites ('histiocytic lymphoma'). This tumor is the most common type seen in mice on the FVB background (>85% of tumors in two large cohorts; Sharpless *et al*., 2001b; Artandi *et al*., 2002). It also occurs, albeit with less frequency, in $p16^{INK4a}$−/− mice, but not in $p19^{ARF}$−/− mice (Table 1). In aggregate, these data imply that $p19^{ARF}$ is an important tumor suppressor in a variety of tissues of mesenchymal, lymphoid, and epithelial origin.

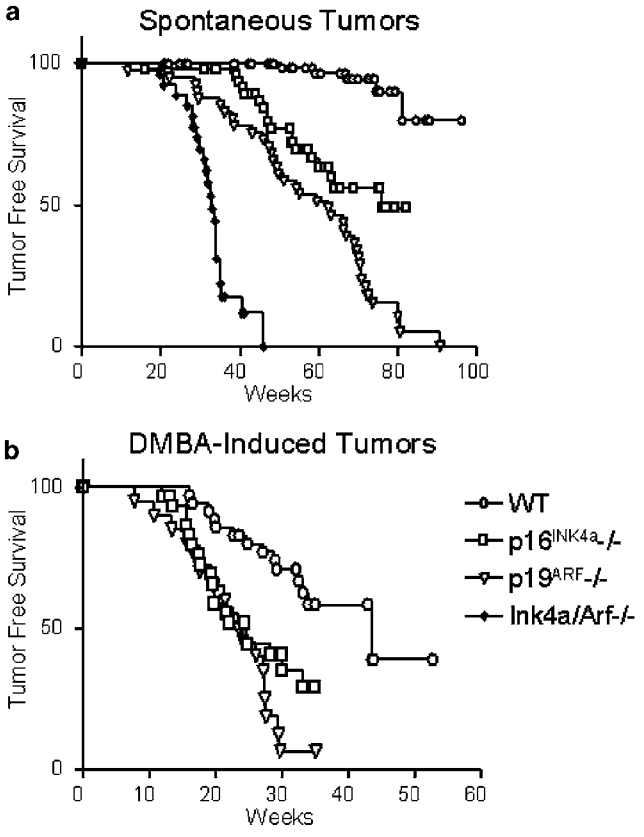

Figure 3 (a, b) Kaplan–Meier analyses of spontaneous (**a**) and DMBA-induced (**b**) tumors in $p19^{ARF}$−/− mice compared to wild-type (WT), $p16^{INK4a}$−/−, and *Ink4a/Arf*−/− mice. In (**b**), $n=78$ mice for WT; 50 for $p16^{INK4a}$−/−; 41 for $p19^{ARF}$−/−; and 21 for *Ink4a/Arf*−/−. In (**b**), $n=35$ mice for WT; 30 for $p16^{INK4a}$−/−; and 20 for $p19^{ARF}$−/−

Single-dose treatment with the potent carcinogen DMBA, on the other hand, produced similar tumor spectra in wild-type, $p16^{INK4a}$−/−, and $p19^{ARF}$−/− mice. Animals of all three backgrounds demonstrated predominantly lymphoma, spindle cell tumors, and lung tumors (Table 1), although the latency was much shorter in $p16^{INK4a}$−/− or $p19^{ARF}$−/− animals (Figure 3b). While mice lacking $p16^{INK4a}$−/− developed proportionally fewer lymphocytic lymphomas than either wild-type or $p19^{ARF}$−/− animals, they instead demonstrated an increased incidence of spindle cell neoplasms after DMBA, a tumor type to which they are also more prone to develop spontaneously. The only tumor type that was unique to a particular genotype after DMBA exposure was the finding of a low frequency of melanoma in $p16^{INK4a}$−/− animals, as has been previously reported (Krimpenfort *et al*., 2001; Sharpless *et al*., 2001a). Intriguingly, while $p19^{ARF}$−/− lung tumors

Table 1 Spontaneous and DMBA-induced tumor spectra by genotype

	Spontaneous			*DMBA-induced*	
WT ($n=4$ tumors)	Malig. sp. cell Neo.	50%	WT ($n=13$ tumors)	Small lymph. lymph.	69%
	Lung CA	50%		Malig. sp. cell neo.	15%
				Lung CA	15%
$p19^{ARF}$−/− ($n=33$ tumors)	Small lymph. lymph.	33%	$p19^{ARF}$−/− ($n=20$ tumors)	Small lymph. lymph.	60%
	Malig. sp. cell neo.	30%		Lung CA	40%
	Lung CA	12%		Malig. sp. cell neo.	15%
	Osteosarcoma	9%			
	Carcinoma (?HCC, other)	6%			
	Neuro. syndrome	9%			
$p16^{INK4a}$−/− ($n=17$ tumors)	Malig. sp. cell neo.	29%		Small lymph. lymph.	40%
	Angiosarcoma	23%	$p16^{INK4a}$−/− ($n=20$ tumors)	Malig. sp. cell neo.	30%
	Osteosarcoma	18%		Lung CA	30%
	Histiocytic lymphoma	18%		Melanoma	5%
	Melanoma	12%			
Ink4a/Arf−/− ($n=21$ tumors)	Histiocytic lymphoma	90%	Ink4a/Arf−/−	Not determined, comparable colony followed by Serrano *et al*. (1996)	
	Malig. sp. cell neo.	9%			

As cohorts were not followed for equal lengths of time, the tumor incidences are shown as the percentage of the total number of tumors analysed. The total number of tumors per genotype is indicated

were larger (7.8 versus 28.7 mm^2, $P=0.04$) and more likely to cause morbidity (e.g. tachypnea, hemothorax) than in wild-type littermate animals; the number of tumor nodules seen in *p19^{ARF}*−/− was not significantly increased, in contrast to *p16^{INK4a}* −/− mice (Sharpless *et al*., 2001a). These data are most consistent with the notion that both p16^{INK4a} and p19^{ARF} inhibit DMBA-induced tumors in largely the same cell types, but with distinct mechanisms of action.

Discussion

We have described the generation of a novel p19^{ARF} specific knockout strain and its comparison to *p16^{INK4a}*, *Ink4a/Arf*, and *p53* deficient animals. The phenotypes of these *p19^{ARF}*−/− mice and cells are similar to those observed in a previously described p19^{ARF} knockout from the Sherr lab (*p19^{ARF} CS*) (Kamijo *et al*., 1997, 1999). Cells from this *p19^{ARF}*−/− strain, however, demonstrate normal p16^{INK4a} expression at early passage compared to littermate *p19^{ARF}*+/+ animals, while cells from the previously described strain demonstrate a several-fold increase in p16^{INK4a} expression (Kamijo *et al*., 1997; Lin and Lowe, 2001). This difference likely stems from the targeting strategy, as the *p19^{ARF} CS* mice were generated with a remnant neomycin selection that presumably disrupts the *p19^{ARF}* promoter. This result supports the view that *p16^{INK4a}* expression is reduced, at least in some circumstances, through promoter competition with *p19^{ARF}*, as has previously been suggested (Mao *et al*., 1995; Stone *et al*., 1995).

Also, the strains differ somewhat in their tumor latency. Several groups (Kamijo *et al*., 1997, 1999; Eischen *et al*., 2002; Tolbert *et al*., 2002) have reported following cohorts of the *p19^{ARF} CS* mice for spontaneous tumors; all report median tumor latencies in the 27–49 week range, whereas the strain reported in this series appears to develop tumors ~10–30 weeks later. A possible explanation is that this targeting strategy generates a hypomorphic allele as a transcript encoding the first 11 amino acids of p19^{ARF} is produced. Even in the unlikely event that this transcript is translated, however, previous results suggest that such a small fragment of p19^{ARF} could not bind mdm2, could not stabilize p53, and would not cause growth arrest in cells (Pomerantz *et al*., 1998; Weber *et al*., 2000; Korgaonkar *et al*., 2002). Along these lines, MEFs from this *p19^{ARF}* knockout strain do not exhibit evidence of intact p19^{ARF} function *in vitro* (Figures 1d, e and 2a–c). Another possible explanation for these differences is that the increased expression of p16^{INK4a} seen in the *p19^{ARF} CS* knockout could contribute to the differences in phenotype. While it seems paradoxical that the strain with increased p16^{INK4a} expression *in vitro* also demonstrates increased tumorigenesis *in vivo*, it is possible that developmental p16^{INK4a} overexpression might select for compensatory epigenetic events that attenuate the Rb pathway function. Finally, these differences between the *p19^{ARF}*-deficient strains could result from differences in environment or genetic background (e.g. FVB versus C57Bl/6).

In accordance with the Sherr group (Kamijo *et al*., 1997), we have demonstrated that most of the *in vitro* phenotypes identified in *Ink4a/Arf*−/− MEFs are the result of p19^{ARF} deficiency. That is, transformation by c-Myc and H-Ras, improved growth at low density, and enhanced growth by 3T9 assay are all seen in *p19^{ARF}*−/− MEFs, to an extent comparable to that seen in *Ink4a/Arf*−/− cells. Therefore, p16^{INK4a} only seems to become an important determinant of MEF growth when highly expressed (e.g. at late passage when p16^{INK4a} loss facilitates immortalization (Sharpless *et al*., 2001a)), or in the setting of reduced p19^{ARF} expression (e.g. growth at high density (Sharpless *et al*., 2002)). In contrast to MEFs, however, p16^{INK4a} has been noted to be a more significant determinant of the *in vitro* growth of murine lymphocytes, macrophages, and astrocytes (summarized in Table 2; Randle *et al*., 2001; Sharpless *et al*., 2001a; Bachoo *et al*., 2002; and Sachs *et al*., in submission). Furthermore, there are extensive data to suggest that p16^{INK4a} plays a more important role in regulating the growth of a variety of human cell types (Brenner *et al*., 1998; Foster *et al*., 1998; Huschtscha *et al*., 1998;

Table 2 The *in vitro* and *in vivo* effects of p16^{INK4a}, p19^{ARF}, and p53 deficiency

Cell culture	*WT*	*p16^{INK4a}*	*p19^{ARF}*	Ink4a/Arf	*p53*	*p16^{INK4a}/p53*
MEF transformation by H-Ras	No	No	Yes	Yes	Yes	Yes
Low-density seeding (number foci)	0–2	0–2	35–60	40–60	>50	ND
Growth at confluence (fold increase over WT)	1.0	1.4	1.0	1.5	ND	ND
Immortalization frequency of MEFs	10%	70%	100%	100%	100%	100%
Immortalization frequency of astrocytes	0%	0%	38%	100%	100%	ND
Lymphocyte immortalization by v-abl	29%	43%	100%	100%	100%	ND
v-abl-induced crisis in lymphocytes	Yes	Yes	Yes	No	No	ND
In vivo						
Tumor latency – spontaneous (weeks)	>100	76	62	38	16	10
Tumor latency – DMBA (weeks)	44	24	24	12	ND	ND
Tumor latency of melanoma in Tyr-RAS background (weeks)	>100	75	40	24	17	ND
Cooperation with Tyr-RAS and UV light in melanoma	No	No	Yes	ND	ND	ND
Cooperation with activated EGFR in orthotopic GBM	No	No	No	Yes	Yes	ND

ND = not determined, see text for references

Kiyono *et al*., 1998; Zhu *et al*., 1998), whereas the role of $p14^{ARF}$ in these settings is unclear (Munro *et al*., 1999; Wei *et al*., 2001; Rheinwald *et al*., 2002). Therefore, the modest importance of $p16^{INK4a}$ as a determinant of MEF growth appears unusual among primary cell cultures from both human and mouse. A likely explanation for this observation is that even at early passage, MEFs highly express the other INK4-class regulators $p18^{INK4c}$ and $p19^{INK4d}$ (Zindy *et al*., 1997). Therefore, $p16^{INK4a}$ may be a stoichiometrically less important regulator of cdk4/6 activity than these other INK4 proteins in early-passage MEFs.

A compilation of results obtained from *p16*^{INK4a}*−/−*, *p19*^{ARF}*−/−*, *Ink4a/Arf−/−*, *p53−/−*, and *p16*^{INK4a}*/p53* compound null mice and cells is shown in Table 2 (present data; (Sharpless *et al*., 2001a, b, 2002, 2003; Bachoo *et al*., 2002; Kannan *et al*., 2003). All of these experiments were performed on mice in a comparable genetic background (>2 backcrosses to FVB), housed in a common facility, and followed by a single group of observers over a 4-year period. These cellular and organismal data unequivocally demonstrate genetic cooperation between $p16^{INK4a}$ and $p19^{ARF}$ loss, as well as between $p16^{INK4a}$ and p53 loss.

In summary, the issue of which protein encoded by the *Ink4a/Arf* locus encodes tumor-suppressor activity appears definitively resolved by the collective experimental evidence of this report and others (Kamijo *et al*., 1997, 1999; Krimpenfort *et al*., 2001; Sharpless *et al*., 2001a, 2002, 2003; Bachoo *et al*., 2002; Kannan *et al*., 2003). Clearly, $p16^{INK4a}$ and $p19^{ARF}$ participate in distinct antitumor pathways, and there is ample evidence from human and mouse studies for cooperation between the combined loss of both proteins. These results bring into sharp relief, however, the limitations of resistance to culture-induced growth arrest, a phenotype depending on $p19^{ARF}$ in MEFs and $p16^{INK4a}$ in most cultured human cells, as a widely utilized surrogate of cancer-relevant activity. A more likely explanation for the intimate but inconsistent relationship between *in vitro* immortalization and tumorigenesis is that the act of culture and the early stages of tumor formation share common features. That is, nascent tumors *in vivo* likely receive *Ink4a/Arf*-dependent growth-inhibitory signals in response to aberrant or inappropriate proliferation that are similar to the culture-related stimuli that induce $p16^{INK4a}$ and $p19^{ARF}$ *in vitro*.

Methods

Targeting of p19^{arf}

Approximately 17 kb of genomic sequence containing exons 1 and 2 of $p15^{INK4b}$ and exon 1β of $p19^{ARF}$ was subcloned and mapped (Figure 1a). A floxed PGK-neomycin cassette was cloned into a *Bss*HII site within exon 1β of a 4.4 kb *Eco*R1-Acc fragment (Figure 1a), and then a targeting construct generated by three-part ligation of the long arm, the *Eco*R1 fragment with Neo cassette, and pKS containing TK for negative selection. The structure of the targeting vector was confirmed, and it was then electroporated into TC1 cells. Correct targeting was confirmed by Southern blotting (Figure 1b) and PCR (not shown). For Southern analysis, a 250 bp *Apa*L1-*Eco*R1 fragment that was external to the targeting vector was used. Blastocyst injections were performed using homologously targeted ES cells. High-percentage chimeras were then crossed to a Cre-deletor strain (EIIa-CRE; Lakso *et al*., 1996) to remove the selection cassette, and correct excision was confirmed by Southern (not shown), PCR (Figure 1c) and direct sequencing of the targeted allele. PCR was performed using primers that flank the remnant LoxP site: p193L (5′-GTC GCA GGT TCT TGG TCA CT-3′) and p194R (5′-ATG TTC ACG AAA GCC AGA GC-3′). A transcript is weakly expressed from the engineered exon 1β that encodes the first 11 amino acids of $p19^{ARF}$, and then a premature stop codon (not shown).

Mouse colony, histopathology, and cell culture

After Cre-mediated excision of the selection cassette, animals were backcrossed to WT FVB females to remove the Cre transgene. N2 and N3 FVB colonies were then generated by backcrossing *p19*^{ARF}*+/−* animals. Littermate tumor cohorts were monitored a minimum of 3× per week. *Ink4a/Arf*, *p16*^{INK4a}, *p53*, and *p16*^{INK4a}*/p53* cohorts were generated by similar mating schemes of heterozygous intercrosses of animals after backcrossing two to four generations to FVB/n (Taconic). All animals were housed in a common facility, followed by a common group of investigators, and histopathologically analysed in a common way. Data from the *p16*^{INK4a}*−/−* and *Ink4a/Arf−/−* cohorts have been previously published (Sharpless *et al*., 2001b, 2002), although the Kaplan–Meier and tumor spectrum analyses from the *p16*^{INK4a}*−/−* cohort were updated for this work (Figure 2a–c). Histopathological analysis and tumor classification were performed as described (Sharpless *et al*., 2001b, 2002). In three animals killed for neurological symptoms (of 41 *p19*^{ARF}*−/−* in the cohort), the cause of death could not be determined, but they are included in the estimate of median tumor-free survival by Kaplan–Meier analysis (Figure 2a), although it is improbable that these deaths were secondary to cancer. MEFs from all strains were made in an identical manner from day 13.5 embryos of heterozygous intercrosses, as previously described (Sharpless *et al*., 2001a). Cell culture, *in vitro* assays, flow cytometry, and Western blotting were performed as previously described (Sharpless *et al*., 2001a). For Western blotting, the following antibodies were used: $p16^{INK4a}$ (M156, Santa Cruz), $p19^{ARF}$ (Ab80, Novus), p21 (F-5, Santa Cruz), actin (C-11, Santa Cruz) and p53 (CM5, Novocastra). Immunohistochemistry was done as described previously (Rheinwald *et al*., 2002) with some modifications. Briefly, cells were BRDU pulsed for 24 h and fixed in 4% paraformaldehyde at indicated passages, incubated in 0.1% Triton X-100, then treated for 1 h with 0.2 N HCl, and neutralized with 0.1 M sodium borate buffer. Cells were stained using antibodies to BrdU (Roche) and $p19^{ARF}$ (Ab80, Novus) for 1 h. Proteins were visualized by using AlexaFluor562 and 488 Molecular Probes secondary antibodies. For cell counting, >600 cells per genotype were counted from three matched pairs of independent littermate cultures at passage 5–11 and compared with a two-sided Fisher's exact test. DMBA treatment was performed as described (Serrano *et al*., 1996). Almost all animals killed at >15 weeks after DMBA treatment demonstrated pulmonary adenomas, but these tumors were only included in the Kaplan–Meier analysis and tumor spectra (Figure 2b and Table 1) when they contributed to the cause of death (for details, see Sharpless *et al*., 2001a).

Acknowledgements
We wish to thank R Carrasco and B Bachoo for assistance with mouse histopathology; C Torrice, S Alson, Aguirre, S Chan, K Chin, and J Horner for advice and reagents; and C Sherr and T Van Dyke for comments on the manuscript. This work was supported by grants from the Howard Hughes Medical Institute, National Institutes of Health and American Cancer Society. RAD is an American Cancer Society Research Professor. NES is a Sydney Kimmel Foundation for Cancer Research Scholar.

References

Artandi SE, Alson S, Tietze MK, Sharpless NE, Ye S, Greenberg RA, Castrillon DH, Horner JW, Weiler SR, Carrasco RD and DePinho RA. (2002). *Proc. Natl. Acad. Sci. USA,* **99,** 8191–8196.

Bachoo RM, Maher EA, Ligon KL, Sharpless NE, Chan SS, You MJ, Tang Y, DeFrances J, Stover E, Weissleder R, Rowitch DH, Louis DN and DePinho RA. (2002). *Cancer Cell,* **1,** 269–277.

Bardeesy N, Bastian BC, Hezel A, Pinkel D, DePinho RA and Chin L. (2001). *Mol. Cell. Biol.,* **21,** 2144–2153.

Brenner AJ, Stampfer MR and Aldaz CM. (1998). *Oncogene,* **17,** 199–205.

Brookes S, Rowe J, Ruas M, Llanos S, Clark PA, Lomax M, James MC, Vatcheva R, Bates S, Vousden KH, Parry D, Gruis N, Smit N, Bergman W and Peters G. (2002). *EMBO J.,* **21,** 2936–2945.

Eischen CM, Rehg JE, Korsmeyer SJ and Cleveland JL. (2002). *Cancer Res.,* **62,** 2184–2191.

Festing M. (1998). *Mouse Genome Informatics Web Site*. Vol. 2001 The Jackson Laboratory: Bar Harbor, Maine.

FitzGerald MG, Harkin DP, Silva-Arrieta S, MacDonald DJ, Lucchina LC, Unsal H, O'Neill E, Koh J, Finkelstein DM, Isselbacher KJ, Sober AJ and Haber DA. (1996). *Proc. Natl. Acad. Sci. USA,* **93,** 8541–8545.

Foster SA, Wong DJ, Barrett MT and Galloway DA. (1998). *Mol. Cell. Biol.,* **18,** 1793–1801.

Hewitt C, Lee Wu C, Evans G, Howell A, Elles RG, Jordan R, Sloan P, Read AP and Thakker N. (2002). *Hum. Mol. Genet.,* **11,** 1273–1279.

Huot TJ, Rowe J, Harland M, Drayton S, Brookes S, Gooptu C, Purkis P, Fried M, Bataille V, Hara E, Newton-Bishop J and Peters G. (2002). *Mol. Cell. Biol.,* **22,** 8135–8143.

Huschtscha LI, Noble JR, Neumann AA, Moy EL, Barry P, Melki JR, Clark SJ and Reddel RR. (1998). *Cancer Res.,* **58,** 3508–3512.

Hussussian CJ, Struewing JP, Goldstein AM, Higgins PA, Ally DS, Sheahan MD, Clark WH, Jr, Tucker MA and Dracopoli NC. (1994). *Nat. Genet.,* **8,** 15–21.

Kamb A, Gruis NA, Weaver-Feldhaus J, Liu Q, Harshman K, Tavtigian SV, Stockert E, Day III RS, Johnson BE and Skolnick MH. (1994). *Science,* **264,** 436–440.

Kamijo T, Bodner S, van de Kamp E, Randle DH and Sherr CJ. (1999). *Cancer Res.,* **59,** 2217–2222.

Kamijo T, Zindy F, Roussel MF, Quelle DE, Downing JR, Ashmun RA, Grosveld G and Sherr CJ. (1997). *Cell,* **91,** 649–659.

Kannan K, Sharpless NE, Xu J, O'Hagan RC, Bosenberg M and Chin L. (2003). *Proc. Natl. Acad. Sci. USA,* **100,** 1221–1225.

Kiyono T, Foster SA, Koop JI, McDougall JK, Galloway DA and Klingelhutz AJ. (1998). *Nature,* **396,** 84–88.

Korgaonkar C, Zhao L, Modestou M and Quelle DE. (2002). *Mol. Cell. Biol.,* **22,** 196–206.

Krimpenfort P, Quon KC, Mooi WJ, Loonstra A and Berns A. (2001). *Nature,* **413,** 83–86.

Lakso M, Pichel JG, Gorman JR, Sauer B, Okamoto Y, Lee E, Alt FW and Westphal H. (1996). *Proc. Natl. Acad. Sci. USA,* **93,** 5860–5865.

Lin AW and Lowe SW. (2001). *Proc. Natl. Acad. Sci. USA,* **98,** 5025–5030.

Lowe SW and Sherr CJ. (2003). *Curr. Opin. Genet. Dev.,* **13,** 77–83.

Mao L, Merlo A, Bedi G, Shapiro GI, Edwards CD, Rollins BJ and Sidransky D. (1995). *Cancer Res.,* **55,** 2995–2997.

Munro J, Stott FJ, Vousden KH, Peters G and Parkinson EK. (1999). *Cancer Res.,* **59,** 2516–2521.

Olson DC, Marechal V, Momand J, Chen J, Romocki C and Levine AJ. (1993). *Oncogene,* **8,** 2353–2360.

Pomerantz J, Schreiber-Agus N, Liegeois NJ, Silverman A, Alland L, Chin L, Potes J, Chen K, Orlow I, Lee HW, Cordon-Cardo C and DePinho RA. (1998). *Cell,* **92,** 713–723.

Randerson-Moor JA, Harland M, Williams S, Cuthbert-Heavens D, Sheridan E, Aveyard J, Sibley K, Whitaker L, Knowles M, Newton Bishop J and Bishop DT. (2001). *Hum. Mol. Genet.,* **10,** 55–62.

Randle DH, Zindy F, Sherr CJ and Roussel MF. (2001). *Proc. Natl. Acad. Sci. USA,* **98,** 9654–9659.

Rheinwald JG, Hahn WC, Ramsey MR, Wu JY, Guo Z, Tsao H, De Luca M, Catricala C and O'Toole KM. (2002). *Mol. Cell. Biol.,* **22,** 5157–5172.

Rizos H, Puig S, Badenas C, Malvehy J, Darmanian AP, Jimenez L, Mila M and Kefford RF. (2001). *Oncogene,* **20,** 5543–5547.

Serrano M, Lee H, Chin L, Cordon-Cardo C, Beach D and DePinho RA. (1996). *Cell,* **85,** 27–37.

Serrano M, Lin AW, McCurrach ME, Beach D and Lowe SW. (1997). *Cell,* **88,** 593–602.

Sharpless NE, Alson S, Chan S, Silver DP, Castrillon DH and DePinho RA. (2002). *Cancer Res.,* **62,** 2761–2765.

Sharpless NE, Bardeesy N, Lee KH, Carrasco D, Castrillon DH, Aguirre AJ, Wu EA, Horner JW and DePinho RA. (2001a). *Nature,* **413,** 86–91.

Sharpless NE, Ferguson DO, O'Hagan RC, Castrillon DH, Lee C, Farazi PA, Alson S, Fleming J, Morton CC, Frank K, Chin L, Alt FW and DePinho RA. (2001b). *Mol. Cell,* **8,** 1187–1196.

Sharpless NE, Kannan K, Xu J, Bosenberg M and Chin L. (2003). *Oncogene*. (in press).

Sherr CJ. (2001). *Cell,* **106,** 531–534.

Sherr CJ and DePinho RA. (2000). *Cell,* **102,** 407–410.

Stone S, Jiang P, Dayananth P, Tavtigian SV, Katcher H, Parry D, Peters G and Kamb A. (1995). *Cancer Res.,* **55,** 2988–2994.

Sviderskaya EV, Gray-Schopfer VC, Hill SP, Smit NP, Evans-Whipp TJ, Bond J, Hill L, Bataille V, Peters G, Kipling D, Wynford-Thomas D and Bennett DC. (2003). *J. Natl. Cancer Inst.,* **95,** 723–732.

Tolbert D, Lu X, Yin C, Tantama M and Van Dyke T. (2002). *Mol. Cell. Biol.,* **22,** 370–377.

Weber JD, Kuo ML, Bothner B, DiGiammarino EL, Kriwacki RW, Roussel MF and Sherr CJ. (2000). *Mol. Cell. Biol.,* **20,** 2517–2528.

Wei W, Hemmer RM and Sedivy JM. (2001). *Mol. Cell. Biol.,* **21,** 6748–6757.

Zhu J, Woods D, McMahon M and Bishop JM. (1998). *Genes Dev.,* **12,** 2997–3007.

Zindy F, Quelle DE, Roussel MF and Sherr CJ. (1997). *Oncogene,* **15,** 203–211.